Published in final edited form as:
J Biomed Mater Res B Appl Biomater. 2008 April ; 85(1): 140–148. doi:10.1002/jbm.b.30926.

Tribological Evaluation of Nanostructured Diamond Coatings and CoCr against Ultra-High Molecular Weight Polyethylene

Michael R. Hill[1], **Shane A. Catledge**[2], **Valeriy Konovalov**[2], **William C. Clem**[1], **Shafiul A. Chowdhury**[2], **Brandon S. Etheridge**[1], **Andrei Stanishevsky**[2], **Jack E. Lemons**[3], **Yogesh K. Vohra**[2], and **Alan W. Eberhardt**[1]

1 *Department of Biomedical Engineering, University of Alabama at Birmingham, Birmingham, AL*

2 *Department of Physics, University of Alabama at Birmingham, Birmingham, AL*

3 *Department of Prosthodontics, University of Alabama at Birmingham, Birmingham, AL*

Abstract

Background—Some loss of joint prostheses has been attributed to osteolytic phenomena leading to loosening and associated with debris from wear of polyethylene articulating against metal alloys. Reduced polyethylene wear has been reported with ceramics serving as an alternative counterface.

Methods—Nanostructured Diamond (NSD) coatings were deposited onto Ti6A14V by microwave plasma-assisted chemical vapor deposition, with both hydrogen-rich (H-NSD) and helium-rich (He-NSD) feedgas mixtures. Pin-on-disk wear tests of polyethylene against NSD and CoCr were performed in serum lubrication at body temperature. Scanning electron microscopy was used to examine surface morphology, and nanoindentation was used to determine hardness and modulus of the polyethylene pins. Raman spectroscopy, surface roughness, and wettability analyses of NSD coatings were performed.

Results—Raman spectroscopy confirmed sp^2 and sp^3 bonded carbon. No significant differences in wear factors were found between polyethylene on H-NSD, He-NSD, and CoCr, despite higher roughness and friction coefficient for the He-NSD and H-NSD coatings, compared to CoCr. Contact angles for the diamond coatings were reduced following the wear tests, indicating that these surfaces became more hydrophilic. Multiple pimples were observed on pins articulated against CoCr, and a single, large protuberance was observed in polyethylene-on-NSD These features were conjectured to be re-consolidated polyethylene particles. Nanoindentation modulus and hardness of the worn polyethylene surfaces were lower for polyethylene-on-diamond than for polyethylene-on-CoCr.

Conclusions—As a counterface to polyethylene, the NSD coatings produced wear factors comparable to CoCr in the present pin-on-disk tests. Thus, NSD-coated Ti6A14V shows promise for use in joint replacement bearing applications.

Keywords

Bearing surfaces; Nanomaterials/nanophase; coating(s); polyethylene (UHMWPE); wear

Introduction

Functional loss of metal-on-polymer joint replacement devices is known to occur through aseptic loosening of the prosthesis due in part to wear-debris-induced osteolysis.[1] There is a general consensus that adverse tissue response to submicron ultra-high molecular weight polyethylene wear particles is a contributor to this loss.[2–10] As an alternative to metallic components, ceramic materials have been investigated as a counterface to polyethylene. The *in vivo* wear of polyethylene acetabular cups against ceramic femoral heads in total hip

arthroplasty has been shown to be lower than polyethylene against cobalt alloy[11] and other metallic counterfaces.[12–13] Pin-on-disk tests reveal similar wear rates of polyethylene against metallic and ceramic disks having similar surface finish,[14–16] and that ceramic (alumina) counterfaces are more resistant to third body wear from bone cement particles than metallic counterfaces.[17] Damage to both metallic counterfaces by third body wear particles may lead to increased polyethylene wear.[17]

Nanostructured diamond (NSD) and diamond-like carbon (DLC) coatings on metallic substrates have been investigated for use in biomedical implants. Hip simulator studies have shown the wear of polyethylene against DLC coatings to be similar to that of polyethylene-on-alumina.[18–19] NSD coatings have been studied for their potential as wear-resistant coatings in the temporomandibular joint prosthesis.[20–21] These NSD coatings could prove to be more resistant to scratching by third body wear particles, such as bone cement, due to their high hardness.[22]

In the present study, we compared the wear behavior of two distinct NSD films deposited on Ti6A14V using different feedgas mixtures in the microwave plasma-assisted chemical vapor deposition (MPCVD) process. In one process mixture, a hydrogen-rich feedgas was used;[23] the other process mixture was rich in helium.[24] Previous studies have shown a significant decrease in grain size and reduction in surface roughness for the helium-rich feedgas mixture as compared to the hydrogen-rich mixture.[23–25] Combined effects of plasma dilution (increased CH_4/H_2 ratio), enhanced fragmentation of carbon-containing species (such as C_2), and enhanced formation of CN radical, may be responsible for the lower surface roughness for films grown with the helium-rich feedgas mixture. For both process mixtures, the formation of CN radical has been correlated with reduction of grain size and surface roughness, as shown in previous studies within our program.[23–25]

The purpose of this study was to evaluate the tribological properties of the NSD coated Ti6A14V as a counterface to polyethylene and to compare the results to polyethylene-on-CoCr. To achieve this aim, we performed pin-on-disk wear tests and measured wear factors and friction coefficients. Surface characteristics of these materials were assessed using optical profilometry, nanoindentation, scanning electron microscopy and contact angle measurement, pre- and post- wear testing.

Materials and Methods

Materials

Stock Ti6A14V (W. Lorenz, Inc., Jacksonville, FL) manufactured according to ASTM Standard F136[26] was machined into 25.4 mm diameter flat, circular disks. Surface roughness of one representative polished titanium sample was measured from a 2 μm^2 area before diamond deposition using atomic force microscopy (Model: Explorer, Veeco Instruments Inc., NY). The root-mean-squared (RMS) value was 3.5 ± 0.5 nm, based on five separate measurements. Stock CoCr (Biomet, Inc., Warsaw, IN) manufactured according to ASTM Standard F1537[27] was machined into 31.8 mm diameter flat, circular disks. An automatic grinder/polisher (Buehler Ecomet®, Lake Bluff, IL) was used to grind the disks flat with SiC sandpaper of decreasing grit size to 1200, and then polished to a smooth, mirror-like finish with a solution of colloidal silica and hydrogen peroxide on a polishing cloth.

Two methods were used to deposit NSD coatings onto the circular Ti6A14V disks in a 6 kW MPCVD system (Wavemat Corp., Ann Arbor, MI). One method involved feedgas rich in hydrogen, H-NSD, and the other rich in helium, He-NSD (Table 1). Both microwave power and pressure were adjusted to give a substrate temperature of approximately 700°C. Micro-Raman spectroscopy (Dilor XY) was used to probe sp^2 and sp^3 carbon bonding structure in

the NSD coatings. An argon ion laser ($\lambda = 514.5$ nm) was used at 100 mW power in 180 degree backscattering configuration. The laser beam passes through a microscope and is focused on the target using a 100X objective lens. Spectra were collected over 5 minute integration times and a linear background subtraction was performed.

Compression molded ultra-high molecular weight polyethylene irradiated in Argon at 25 – 40 kGy (Arcom®, Biomet, Inc., Warsaw, IN) was machined into cylindrical wear pins 9.50 mm in diameter with a step down to 4.76 +/− 0.03 mm diameter on the contacting surface, giving a contact area of approximately 17.8 mm^2 (Figure 1). At least 0.1 mm of the wear surface was removed with a sledge microtome to eliminate the visible concentric machining marks, leaving a smooth contact surface.[28] The pins were soaked in distilled water for a minimum of two weeks prior to wear testing.

Friction and Wear Testing

Wear tests were conducted in an AMTI OrthoPOD® six station pin-on-disk wear testing machine (Advanced Mechanical Testing, Inc., Watertown, MA), following ASTM Standard F732.[29] Test 1 included four H-NSD Samples with one CoCr sample, and Tests 2 and 3 each included four He-NSD samples with one CoCr sample.

During testing, the samples were contained in a single, large well submerged in lubricant composed of 100% triple 0.1 pm sterile-filtered defined bovine calf serum (Hyclone, Logan, UT) diluted to a total protein concentration of 23 g/L.[30] Sodium azide was added (0.2% w/v) as an antibacterial agent. Anhydrous ethylenediaminetetraacetic acid, or EDTA (Sigma-Aldrich, St. Louis, MO), was added to the serum at 20 mM (7.45 g/L) to bind calcium in solution and minimize the precipitation of abrasives onto the bearing surfaces.[29] The solution was filtered through a 0.22 micrometer filter. The test lubricant was heated to 37°C and maintained at this temperature throughout wear testing. Distilled water was added as needed to account for evaporation.

The wear track followed a square-shaped pattern, 10 mm on a side, such that the polyethylene wear surface changed direction relative to the counterface, which prevents polymer chain alignment and provides more realistic simulation than unidirectional or reciprocating sliding.[31,32] The sliding distance was 40 mm/cycle at a cyclic frequency of 1.5 Hz. The average contact force was 102.0 +/− 1.6 N, giving an average contact stress of 5.71 +/− 0.09 MPa, which is within the range recommended by ASTM Standard F732.[29]

The OrthoPOD® was programmed to record force and coefficient of friction at intervals of 125,000 cycles. At each interval, 200 data points were taken over a 1 second period for each station, and the total number data over the duration of the wear tests (2,000,000 cycles) were averaged to determined force and coefficient of friction. The horizontal (F_x and F_y) and vertical (F_z) force components at the pin-disk interface were measured simultaneously by three separate triaxial load cells. The accuracy of the force measurements were +/− 2N and +/− 8 N for the horizontal and vertical forces, respectively (personal communication, AMTI). The coefficient of friction (μ) for each wear couple was determined as:

$$\mu = \frac{\sqrt{\sum F_x^2 + \sum F_y^2}}{\sum F_z} \quad (1)$$

Each test was carried out for 2 million cycles, or roughly 80 km total sliding distance. Prior to testing and at periodical stops of 0.5 million cycles, the polyethylene pins were cleaned by the method described in ASTM F732.[29] Briefly, the pins were sonically agitated in 1% LiquiNox® (Alconox Inc., White Plains, NY) solution, rinsed in deionized water, and then soaked in ethyl alcohol. A dessicator under vacuum was used for drying. Mass loss was determined by taking

the average of five measurements[28] on a Mettler Toledo AG245 microbalance (Columbus, OH) with resolution to 0.01 mg. During these stops, the well and disks were thoroughly rinsed free of visible lubricant and debris with distilled water, and fresh lubricant was added.

In each test, one non-contacting pin served as a soak control to account for fluid absorption, and the mass loss of each pin was compensated by the mass change of the respective soak control pin. To convert to volume loss, mass loss was divided by the density of polyethylene, 0.933 mg/mm^3, and volume loss was plotted as a function of number of cycles. Volumetric wear rate at 2 million cycles, reported in units of cubic millimeters per million cycles, was calculated by linear regression without the line passing through the origin.[32] A wear factor, k (mm^3/Nm), was determined by dividing the volumetric wear rate by the product of average vertical force and total sliding distance.

Surface Characterization

Three-dimensional surface parameters: arithmetic mean deviation (Sa), root-mean-square deviation (Sq), maximum peak height (Sp), and maximum valley depth (Sv) of the NSD coatings were determined from 5 scans of 0.30 mm^2 areas on each NSD-coated Ti6A14V and CoCr specimen with a Fogale Nanotech optical profilometer (Nimes, France) post-wear testing. The scan areas were taken both within and outside the wear track.

Surface wettability of the NSD coatings was determined by the half angle method using a CAM-MICRO model contact angle meter (Tantec Inc., Schaumburg, IL), with deionized water as the probe liquid. Five separate contact angle measurements were made for each H-NSD (n = 3) and He-NSD (n = 3) specimen, pre- and post-wear testing.

After the 2 million-cycle wear tests, the ends of polyethylene pins which had been in contact with H-NSD, He-NSD, and CoCr were sputter coated with a few nanometers of gold and examined using a scanning electron microscope (SEM; Philips 515, Amsterdam, Netherlands).

In order to measure the hardness and Young's modulus of the polyethylene, nanoindentation measurements were carried out using a Nanoindenter XP (MTS Systems, Oak Ridge TN) system. The system was calibrated by using silica samples for a range of operating conditions. Silica modulus was calculated as 70 GPa. A Berkovich diamond indenter with total included angle of 142.3° was used for all the measurements, which were done using a 350 nm penetration depth. Hold times of 10 seconds at maximum load and 50 seconds at 10 percent of maximum load during unloading were used to compensate for creep and to minimize thermal drift, respectively. The data was processed using proprietary software to produce load-displacement curves and the mechanical properties were calculated using the Oliver and Pharr method.[33]

Statistical Methods

Results were determined in terms of the mean ± one standard deviation. The Kruskal Wallis test was employed to compare average surface parameters, coefficient of friction, and wear factor between H-NSD, He-NSD, and CoCr, with a level of statistical significance, $\alpha = 0.05$. If a significant difference was observed, multiple comparisons were then performed using Man Whitney U tests with the level of significance reduced by the Bonferroni approximation for three comparisons ($\alpha = 0.0167$).

Results

Coating Properties

Micro-Raman spectra ($\lambda = 514.5$ nm) for NSD films grown using $He/H_2/CH_4/N_2$ feedgas mixtures with He contents of 0% (H-NSD) and 71% (He-NSD) of total flow rate show broad

peaks at 1137, 1340, 1485, and 1550 cm^{-1} (Figure 2). These peaks are typically observed for nanostructured diamond films containing sp^2 and sp^3 bonded carbon. The broadening of the peak centered at 1340 cm^{-1} is characteristic of nano-crystalline diamond.[34,35] The broadband centered at 1530 cm^{-1} is primarily associated with tetrahedral amorphous carbon.[36] The Raman spectra have another peak at 1150 cm^{-1} attributed to nanosize diamond crystals.[35] The present NSD films were therefore characterized as diamond nanocrystallites imbedded in a tetrahedral amorphous carbon matrix with a relatively small amount of graphitic carbon. The film grown using helium resulted in a broader 1340 cm^{-1} peak indicative of a reduced diamond grain size and is consistent with our previous measurements.[24]

Friction and Wear

Polyethylene-on-CoCr displayed the lowest coefficient of friction, followed by He-NSD, then H-NSD (Figure 3a; $p < 0.004$, Kruskal Wallis). Individually, CoCr had a lower coefficient of friction than He-NSD and H-NSD ($p < 0.03$, Ma n-Whitney U). Also, the coefficient of friction for He-NSD was lower than that of H-NSD ($p < 0.0$ 07, Man-Whitney U).

The change in mass, due to fluid absorption, of the soak control pins averaged 0.1 +/− 0.5 mg. The mass loss of each pin was adjusted with the mass change of the soak control pin in its respective wear test. Polyethylene exhibited less wear against four H-NSD samples (n = 4, Test 1) and five He-NSD samples (n = 2, Test 2; n = 3, Test 3), as compared to CoCr in each respective test. The average wear factors for both NSD coatings were each lower than that of CoCr (Figure 3b), although the differences were not significant ($p = 0.16$; Kruskal Wallis)

Surface Characteristics

Three-dimensional surface profiles of H-NSD, He-NSD and CoCr reveal differences in surface morphology (Figure 4). No differences were apparent between scans taken within and outside the wear track. For each of the 3-D surface parameters (Sa, Sq, Sp, Sv), CoCr exhibited the lowest average value followed in increasing order by He-NSD and H-NSD (Figure 5; $p < 0.0001$, Kruskal Wallis). Multiple comparisons revealed that all four parameters for He-NSD and H-NSD were both significantly higher than those for CoCr ($p < 0.009$, Man Whitney U). Furthermore, Sa, Sq, and Sp for He-NSD were significantly lower than for H-NSD ($p < 0.0002$, Man Whitney U), but not for Sv ($p = 0.28$, Man Whitney U).

Unworn samples of He-NSD and the H-NSD produced contact angles of 82.3 ± 4.9 and 86.2 ± 9.7 degrees respectively. After wear tests, the H-NSD and He-NSD disc surfaces produced an average contact angle 61.4 ± 8.0 degrees, demonstrating over 25% reductions in contact angle following wear testing and indicating increased hydrophilic behavior.

The SEM images revealed noticeable differences in the surface morphology of the polyethylene pins articulating against CoCr versus those against H-NSD and He-NSD. After all three wear tests, multiple protuberances (pimples) were visible on the surface of the pins that were in contact with CoCr (Figure 6a). A single, large, elevated protuberance appeared on the surface of the pins that were in contact with NSD coatings (Figure 7). Under higher magnification, these elevated regions were revealed as accumulations of polyethylene atop areas of ripples and pulled out fibers (Figure 6b–d). Nanoindentation modulus and hardness of the worn polyethylene surfaces were E = 0.58 ± 0.10 GPa and H = 0.037 ± 0.006 GPa, respectively, for polyethylene-on-diamond. For polyethylene-on-CoCr, the values were E = 0.77 ± 0.085 GPa and H = 0.045 ± 0.02 GPa. In each case, the results were similar for indentation sites within or outside of the visible protuberances. Nanoindentation of an unworn pin produced average values of E = 0.81 ± 0.1 GPa and H = 0.037 ± 0.007 GPa.

Discussion

The average wear factor calculated for polyethylene-on-CoCr ($k = 5.7 +/- 0.8 \times 10^{-7}$ mm^3/Nm) falls within the range determined from retrieval studies of total hip replacements ($k = 9.0 \times 10^{-8} - 7.2 \times 10^{-6}$ mm^3/Nm).[37] This result suggests that the current wear testing protocol was reasonable for a comparative study of polyethylene wear against various counterfaces.

In the present tests, where flat ended pins were worn against the various surfaces in a square pattern under nearly constant loading, polyethylene experienced the lowest average volumetric wear against the H-NSD surfaces, with increasing values for He-NSD and CoCr, respectively. The results were in contrast to higher average roughness values and coefficients of friction exhibited by the polyethylene-NSD wear couples as compared to polyethylene on CoCr. This phenomenon was previously observed in a hip simulator study.[38] Although the differences in wear between groups were not statistically significant, nine of the twelve NSD samples exhibited wear factors less than or equal to the lowest value obtained for CoCr ($k = 4.8 \times 10^{-7}$ mm^3/Nm). Additional wear tests that run to 3- or 4-million cycles are warranted, which may better reveal differences in the long term wear behavior. In addition, different polyethylene types should be included in future wear studies of NSD coated substrates.

Examination of the pins revealed some similarities between the polyethylene wear surfaces articulated against the various counterfaces. Under SEM, a rippled surface with pulled-out and torn fibrils were observed in polyethylene-on-CoCr across the surface area surrounding the pimples (Figures 6c,d) and in polyethylene-on-NSD in areas surrounding the large central protuberance. Similar wear characteristics of polyethylene have been observed previously, where fibril formation was attributed to micro-adhesive wear[39] and the source of the rippled polyethylene was micro-fatigue.[40]

A visible difference between the pin surfaces that articulated against NSD versus CoCr was the size and distribution of raised areas of polyethylene resembling “pimples” or “protuberances.” Small, scattered pimples were noted previously with polyethylene-on-CoCr in an OrthoPOD®, but their source was not determined.[41] Others described such features as areas of higher wear resistance that rose above the surrounding area when the applied load was removed.[42] Closer inspection of the protuberances observed in the present study suggests that they were clusters of polyethylene debris that had been torn from the surface and subsequently reattached in clumps, consistent with the mechanism proposed in a previous hip simulator study.[43] To the authors’ knowledge, this phenomenon has not been reported clinically and may, therefore, indicate a limitation with this and other *in vitro* wear studies. Had the worn polyethylene not re-attached itself to the articulating pin surface, the resulting wear coefficients may have been substantially different. Nanoindentation revealed that the polyethylene-on-diamond contact resulted in reduced modulus of the polyethylene pin surface, in and around the wear-scar, as compared to polyethylene-on-CoCr. This result may be related to differences in surface damage/fibril pullout and subsequent work-hardening or changes in crystallinity of the polyethylene when articulated against these materials.

There was no significant difference in measured contact angle between H-NSD and He-NSD samples, before or after wear testing against polyethylene. However, there was a significant reduction in contact angle (becomes more hydrophilic) after the NSD samples were worn against polyethylene. This is likely due to the presence of a surface film composed of polyethylene and/or serum proteins. Adsorption and saturation of the surface by proteins was observed previously following immersion of CoCr alloys and stainless steel in 50% bovine calf serum, as indicated by the reduction of contact angle with time.[44] Surface hydrophilicity of the sliding surfaces in a hip implant can have a major effect on both protein adsorption and frictional behavior.[45] Since the present NSD coatings were indistinguishable in terms of

surface wettability, we cannot conclude that wettability had a significant effect on wear or lubrication properties between the diamond coatings. It was clear, however, that once the NSD surfaces were coated with polyethylene and/or serum proteins, they became more hydrophilic.

As seen previously,[41] the appearance of the lubricant in this studychanged after only a few thousand wear cycles. Initially, the serum bath was translucent and exhibited a reddish-brown tint. As the wear test progressed, however, it turned to a creamy yellow color and increased in opacity. Upon removal of the lubricant at each weighing stop at 500,000-cycle intervals, a white film was evident on the horizontal surfaces of the lubricant reservoir, including the surfaces of the disks, except for a small circular area where the pin had rested. The white film was likely formed by the precipitation of soluble proteins from the lubricant during wear testing.[41]

Two possible outcomes resulting from this protein precipitation have been previously hypothesized. A film of precipitated protein may have formed a solid lubricant layer between the pins and disks.[30,46] Increases in protein precipitation, caused by the elevation of local serum temperatures due to increased friction, may have been responsible for reductions in wear. In a hip simulator study,[47] protein precipitation was observed in a diluted bovine serum lubricant (54 mg/mL) when the temperature increased above 60°C. Wear rates were found to be inversely related to precipitation, with the highest polyethylene wear against alumina, followed by CoCr and then zirconia. Higher maximum temperatures were calculated for a zirconia ball against a polyethylene cup (99°C), followed by CoCr (60°C), and then alumina (45°C).[46]

Alternatively, the loss of soluble proteins may have reduced the lubricity of the bovine serum with a detrimental influence on the wear behavior of polyethylene.[46] This result in turn may have led to the formation of the presentprotuberances, despite the initial lubricant protein concentration (23 mg/mL) being above the 20 mg/mL threshold for protuberance formation given previously.[30] To date, neither hypothesis has been confirmed, since the specific proteins responsible for boundary lubrication in bovine serum have yet to be identified.[48]

In summary, pin-on-disk wear testing was used presently to evaluate nanostructured diamond coated Ti6A14V against ultra-high molecular weight polyethylene, in comparison to CoCr. The results indicated that the NSD coatings show promise for potential use in joint prostheses. One potential benefit of the diamond coatings may be their inherent the resistance to third-body damage due to their high hardness values (e.g., H = 58 – 72 GPa for He-NSD);[24] therefore, future third-body wear tests are warranted. While pin-on-disk wear testing is an appropriate screening tool for candidate materials, simulator studies should be used to confirm the trends observed presently. Further investigation into the role of protein concentration and precipitation on the formation of the different polyethylene surface features may provide insight into the wear mechanisms and confirm that NSD-coated Ti6A14V may be a suitable alternative to cobalt alloy in total joint prostheses.

Acknowledgements

Support for this study was provided by the National Institute of Dental and Craniofacial Research (NIDCR), the National Institutes of Health (NIH) under Grant No. R01 DE013952-06, the National Science Foundation (NSF) Graduate Research Fellowship Program (GRFP), the Department of Biomedical Engineering and the Department of Physics at the University of Alabama at Birmingham. We are grateful to W. Lorenz, Inc. (Jacksonville, FL) and Biomet, Inc. (Warsaw, IN) for providing materials. Finally, we thank Gerald McGwin for his assistance in the statistical analyses.

References

1. Willert HG, Semlitsch M. The Classic: Tissue reactions to plastic and metallic wear products of joint endoprotheses. Clin Orthop Rel Res 1996;333:4–14.
2. Tipper JL, Ingham E, Hailey JL, Besong AA, Fisher J, Wroblewski BM, Stone MH. Quantitative analysis of polyethylene wear debris, wear rate, and head damage in retrieved Charnley hip prostheses. J Mat Sci: Mat Med 2000;11:117–124.
3. Kadoya Y, Revell PA, Kobayashi A, Al-Saffar N, Scott G, Freeman MAR. Wear particulate species and bone loss in failed total joint arthroplasties. Clin Orthop Rel Res 1997;340:118–129.
4. Harris WH. The problem is osteolysis. Clin Orthop Rel Res 1995;311:46–53.
5. Harris WH. Osteolysis and particle disease in hip replacement. Acta Orthop Scand 1994;65:113–123. [PubMed: 8154274]
6. Amstutz HC, Campbell P, Kossovsky N, Clarke 1C. Mechanism and clinical significance of wear debris-induced osteolysis. Clin Orthop Rel Res 1992;276:7–18.
7. Schmalzried TP, Kwong LM, Jasty M, Sedlacek RC, Haire TC, O'Connor DO, Bragdon CR, Kabo JM, Malcolm AJ, Harris WH. The mechanism of loosening of cemented acetabular components in total hip arthroplasty: analysis of specimens retrieved at autopsy. Clin Orthop Rel Res 1992;274:60–78.
8. Willert HG, Bertram H, Buchorn GH. Osteolysis in alloarthroplasty of the hip: the role of ultra-high molecular weight polyethylene wear particles. Clin Orthop Rel Res 1990;258:95–107.
9. Howie DW, Vernon-Roberts B, Oakeshott R, Manthey B. A rat model of resorption of bone at the cement-bone interface in the presence of ultra-high molecular weight polyethylene acetabular cups. J Bone Joint Surg 1988;70:257–263. [PubMed: 3257760]
10. Revell PA, Weightman B, Freeman MA, Roberts BV. The production and biology of polyethylene wear debris. Arch Orthop Trauma Surg 1978;91:167–181. [PubMed: 666546]
11. Schuller HM, Marti RK. Ten-year socket wear in 66 hip arthroplasties: ceramic versus metal heads. Acta Orthop Scand 1990;61:240–243. [PubMed: 2371818]
12. Zichner L, Lindenfeld T. In vivo wear of the slide combinations ceramics-polyethylene as opposed to metal-polyethylene. Orthopade 1997;26:129–134. [PubMed: 9157352]
13. Oonishi H, Takayaka Y, Clarke 1C, Jung H. Comparative wear studies of 28-mm ceramic and stainless steel total hip joints over 2 to 7 year period. J Long-Term Effects of Medical Implants 1992;2:37–47.
14. Lancaster JG, Dowson D, Isaac GH, Fisher J. The wear of ultra-high molecular weight polyethylene sliding on metallic and ceramic counterfaces representative of current femoral surfaces in joint replacement. Proc Inst Mech Eng (H): J Eng Med 1997;211:17–24.
15. Weightman B, Light D. The effect of surface finish on alumina and stainless steel on the wear rate of UHMW polyethylene. Biomaterials 1986;7:20–24. [PubMed: 3955153]
16. McKellop H, Clarke I, Markolf K, Amstutz H. Friction and wear properties of polymer, metal, and ceramic prosthetic joint materials evaluated on a multichannel screening device. J Biomed Mater Res 1981;15:619–653. [PubMed: 12659132]
17. Cooper JR, Dowson D, Fisher J, Jobbins B. Ceramic bearing surfaces in total artificial joints: resistance to third body wear damage from bone cement particles. JMedEngTech 1991;15:63–67.
18. Saikko V, Ahlroos T, Calonius O, Keranen J. Wear simulation of total hip prostheses with polyethylene against CoCr, alumina and diamond-like carbon. Biomaterials 2001;22:1507–1514. [PubMed: 11374449]
19. Affatato S, Frigo M, Toni A. An in vitro investigation of diamond-like carbon as a femoral head coating. J Biomed Mat Res B: Appl Biomater 2000;53B:221–226.
20. Fries MD, Vohra YK. Nanostructured diamond film deposition on curved surfaces of metallic temporomandibular joint implant. J Phys D: Appl Phys 2002;35:L105–L107.
21. Papo MJ, Catledge SA, Vohra YK, Machado C. Mechanical wear behavior of nanocrystalline and multicrystalline diamond coatings on temporomandibular joint implants. J Mater Sci: Mat Med 2004;15:773–777.

22. Catledge SA, Borham J, Vohra YK, Lacefield WR, Lemons JE. Nanoindentation hardness and adhesion investigations of vapor deposited nanostructured diamond films. J Appl Phys 2002;91:5347–5352.
23. Catledge SA, Vohra YK. Effect of nitrogen addition on the microstructure and mechanical properties of diamond films grown using high-methane concentrations. J Appl Phys 1999;86:698–700.
24. Konovalov VV, Melo A, Catledge SA, Chowdhury S, Vohra YK. Ultra-smooth nanostructured diamond films deposited from He/H2/CH4/N2 microwave plasmas. J Nanosci Nanotech 2006;6:1–4.
25. Corvin RB, Harrison JG, Catledge SA, Vohra YK. Gas-phase thermodynamic models of nitrogen-induced nanocrystallinity in chemical vapor-deposited diamond. Appl Phys Lett 2002;80:2550–2552.
26. ASTM F136 - 02a. Standard specification for wrought titanium - 6 aluminum -4 vanadium ELI (extra low interstitial) alloy for surgical implant applications (UNS R56401). Philadelphia, PA: 2003. p. 269-278.
27. ASTM F1537 - 00. Standard specification for wrought cobalt - 28 chromium - 6 molybdenum alloys for surgical implants (UNS R31537, UNS R31538, and UNS R31539). Philadelphia, PA: 2003. p. 269-278.
28. Barbour PSM, Stone MH, Fisher J. A study of the wear resistance of three types of clinically applied UHMWPE for total replacement hip prostheses. Biomaterials 1999;20:2101–2106. [PubMed: 10555077]
29. ASTM F732 - 00. Standard test method for wear testing of polymeric materials used in total joint prostheses. Philadelphia, PA: 2003. p. 269-278.
30. Saikko V. Effect of lubricant protein concentration on the wear of ultra-high molecular weight polyethylene sliding against a CoCr counterface. J Tribology 2003;125:638–642.
31. Saikko V, Calonius O, Keranen J. Effect of slide track shape on the wear of ultra-high molecular weight polyethylene in a pin-on-disk wear simulation of total hip prosthesis. J Biomed Mat Res B: Appl Biomater 2004;69B:141–148.
32. Bragdon CR, O'Connor DO, Lowenstein JD, Jasty M, Syniuta WD. The importance of multidirectional motion on the wear of polyethylene. Proc Instn Mech Engrs (H): J Eng Med 1996;210:157–165.
33. Oliver WC, Pharr GM. An improved technique for determining hardness and elastic modulus using load and displacement sensing indentation experiments. Journal of materials research 1992;7(6): 1564–1583.
34. Gruen DM, Krauss AR, Zuiker CD, Csencsits R, Terminello LJ, Carlisle JA, Jimenez I, Sutherland DGJ, Shuh DK, Tong W, Himpsel FJ. Characterization of nanocrystalline diamond films by core-level photoabsorption. Appl Phys Lett 1996;68:1640.
35. Nemanich J, Glass JT, Lucovsky G, Shroder RE. Raman scattering characterization of carbon bonding in diamond and diamondlike thin films. J Vac Sci Technol A 1988;6:1783.
36. Friedmann TA, Sulli van JP, Knapp JA, Allant DRT, Follstaedt DM, Medlin DL, Mirkarimi PB. Thick stress-free amorphous-tetrahedral carbon films with hardness near that of diamond. Appl Phys Lett 1997;71:3820.
37. Atkinson J, Dowson D, Wroblewski B. Laboratory wear tests and clinical observations of the penetration of femoral heads into acetabular cups in total replacement hip joints. III. The measurement of internal volume changes in explanted Charnley sockets after 2–16 years in vivo and the determination of wear factors. Wear 1985;104:225–244.
38. Lu Z, McKellop H, Liao P, Benya P. Potential Thermal Artifacts in Hip Joint Wear Simulators. J Biomed Mat Res B: Appl Biomater 1999;48B:458–464.
39. McKellop HA, Campbell P, Park S-H, Schmalzried TP, Grigoris P, Amstutz HC, Sarmiento A. The origin of submicron polyethylene wear debris in total hp arthroplasty. Clin Orthop Rel Res 1995;311:3–29.
40. Wang A, Stark C, Dumbleton JH. Role of cyclic plastic deformation in the wear of UHMWPE acetabular cups. J Biomed Mat Res 1995;29:619–626.
41. Mazzucco D, Spector M. Effects of contact area and stress on the volumetric wear of ultrahigh molecular weight polyethylene. Wear 2003;254:514–522.

42. Saikko V, Ahlroos T. Wear simulation of UHMWPE for total hip replacement with a multidirectional motion pin-on-disk device: effects of counterface material, contact area, and lubricant. J Biomed Mat Res 2000;49:147–154.

43. Tateiwa T, Clarke I, Shirasu H, Masaoka T, Shishido T, Yamamoto K. Effect of low protein concentration lubricants in hip simulators. J Orthop Sci 2006;11:204–211. [PubMed: 16568395]

44. Yan Y, Neville A, Dowson D. Biotribocorrosion - an appraisal of the time dependence of wear and corrosion interactions: II. Surface analysis. J Phys D: Appl Phys 2006;39:3206–3212.

45. Widmer MR, Heuberger M, Spencer ND. Influence of Polymer Surface Chemistry on Frictional Properties Under Protein-Lubrication Conditions. Trib Lett 2001;10:111–116.

46. Lu Z, McKellop H. Frictional heating of bearing materials tested in a hip joint wear simulator. Proc Instn Mech Engrs (H): J Eng Med 1997;211:101–108.

47. Liao Y-S, Benya PD, McKellop HA. Effect of protein lubrication on the wear properties of materials for prosthetic joints. J Biomed Mat Res B: Appl Biomat 1999;48B:465–473.

48. Mazzucco D, Spector M. The John Charnley Award paper: the role of joint fluid in the tribology of total joint arthroplasty. Clin Orthop Rel Res 2004;429:17–32.

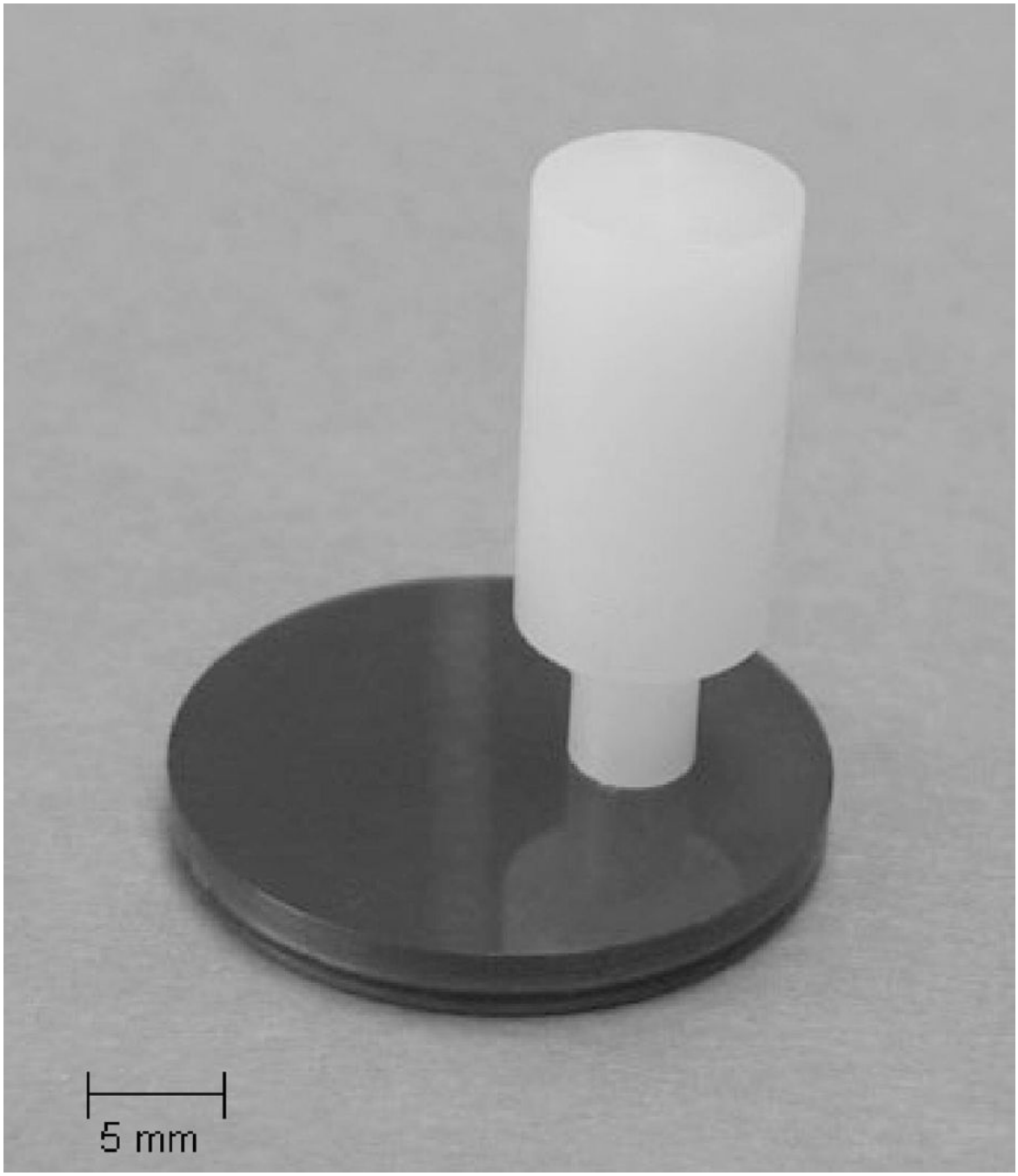

Figure 1.
Ultra-high molecular weight polyethylene pin on a NSD-coated Ti6A14V disk.

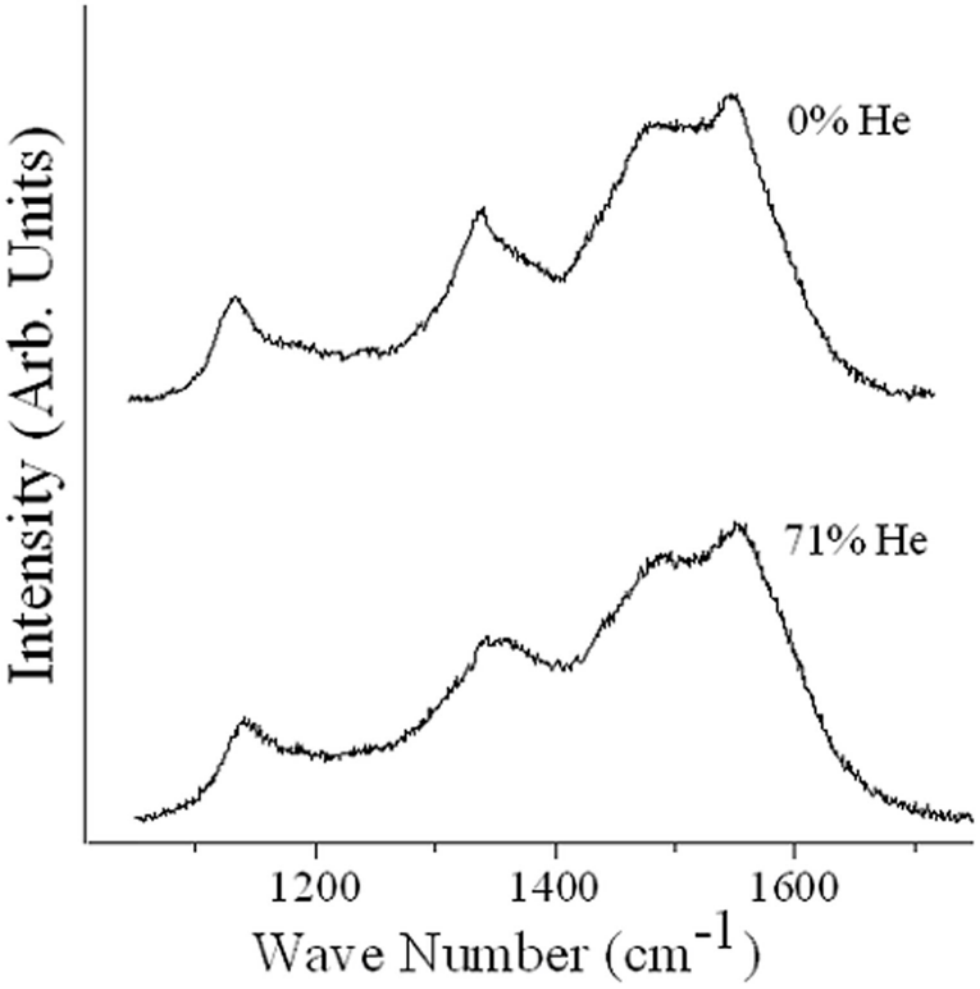

Figure 2.
Micro-Raman spectra (λ, = 514.5 nm) for NSD films grown using $He/H_2/CH_4/N_2$ feedgas mktures with He contents of 0% (H-NSD) and 71% (He-NSD) of total flow rate.

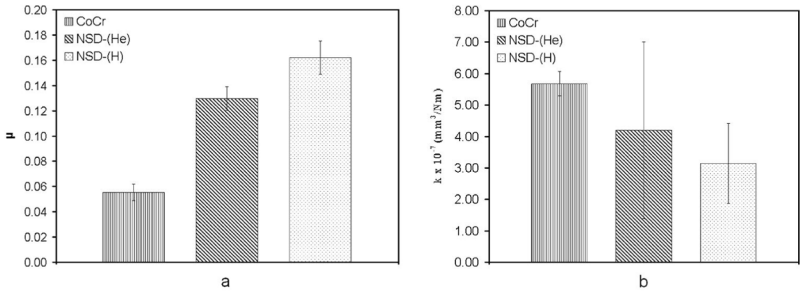

Figure 3.

(a) Coefficient of friction between PE and CoCr, He-NSD and H-NSD (b) Average wear factor for PE on CoCr, He-NSD and H-NSD Error bars represent one standard deviation.

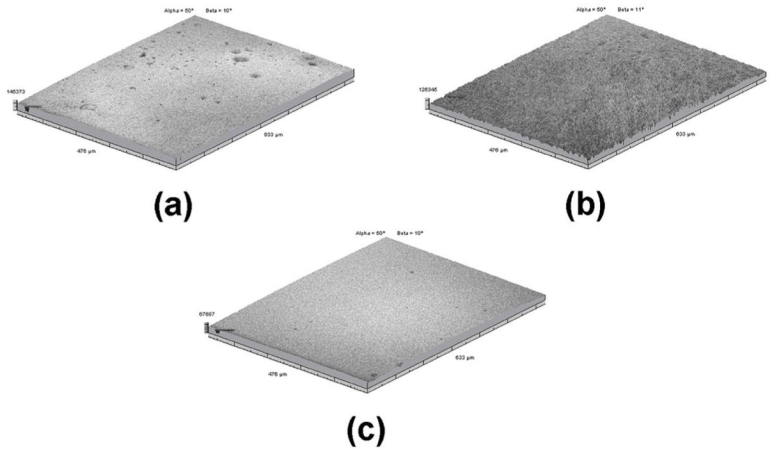

Figure 4.

Images, taken with the optical profilometer, of the sample surfaces, (a) He-NSD, (b) H-NSD and (c) CoCr. Notice the smaller z-direction scale bar of (c) compared to (a) and (b), indicative of a much smoother polished CoCr surface.

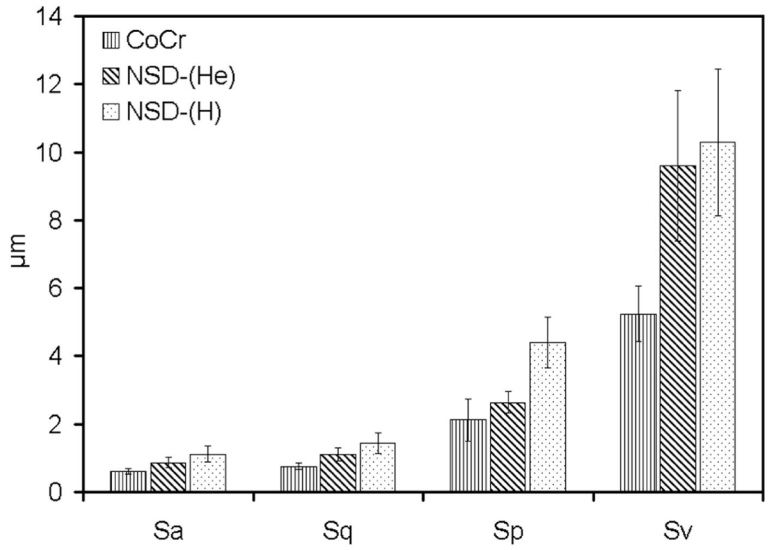

Figure 5.
Three-dimensional surface parameters, measured with the optical profilometer, for CoCr, He-NSD, and H-NSD. Error bars represent one standard deviation.

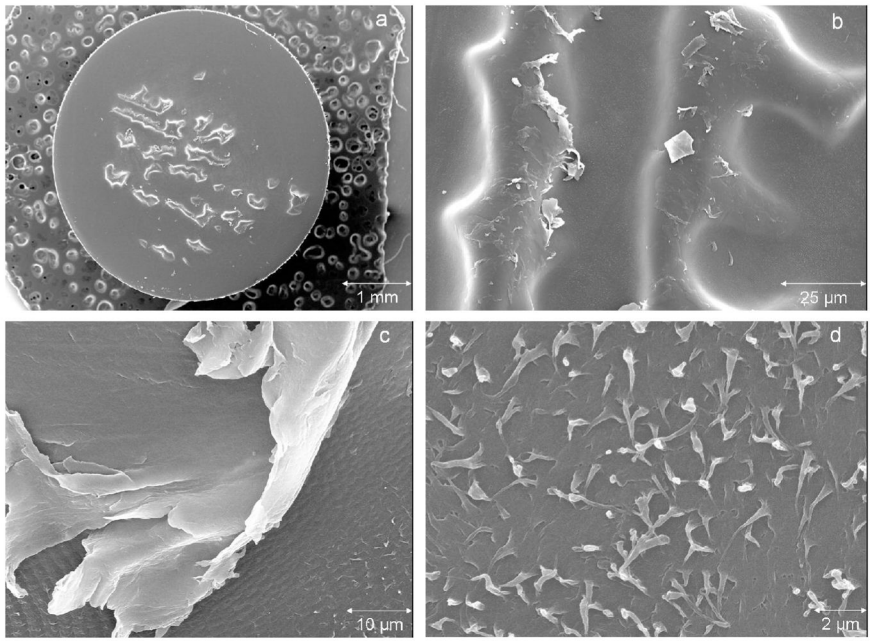

Figure 6.

Scanning electron micrographs of the worn surface of a polyethylene pin after articulating against CoCr for 2 million cycles, (a) At26.4X magnification multiple protuberances appear scattered across the surface, (b) At1,600X magnification, protuberances appear to be areas of elevated polyethylene surrounded by a sea of rippled polyethylene. Large flakes appear to be delaminating from the surface of the protuberances, (c) At 2,500X, the edge of a protuberance appears to be delaminating from the surface. Also, notice the ripples and fibrils on the surface surrounding the protuberance, (d) At 10,000X magnification, pulled-out fibrils can be seen on the rippled surface, indicative of micro-adhesive wear.

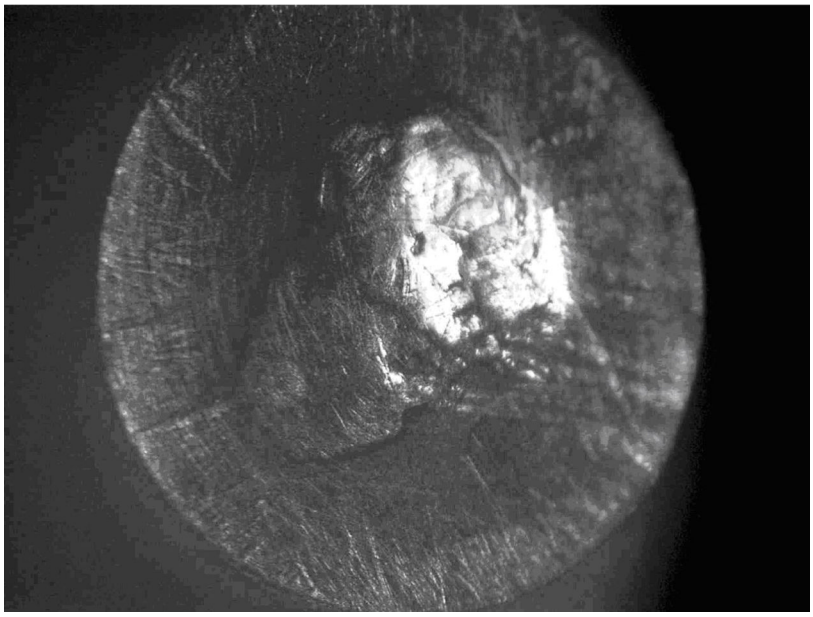

Figure 7.
Stereomicroscope image of the worn surface of a polyethylene pin after articulating against NSD for 2 million cycles, revealing a large, elevated protuberance in the center of the pin. The single protuberance was surrounded by rippled polyethylene similar to images presented in Figure 6b–d.